Kocatepe Veterinary Journal

Kocatepe Vet J (2025) 18(3):311-320
DOI: 10.30607/kvj.1718885

RESEARCH ARTICLE

3D Reconstruction of Some Limb Bones in New Zealand Rabbits with 3D Scanning and Computed Tomography: Morphological Investigation

Ali KOÇYİĞİT[1*], Mustafa Orhun DAYAN[2], Mustafa KOPLAY[3]

[1]Laboratory and Veterinary Health Vocational School, Harran University, Şanlıurfa, Türkiye
[2]Department of Anatomy, Faculty of Veterinary Medicine, Selçuk University, Konya, Türkiye
[3]Department of Radiology, Faculty of Medicine, Selçuk University, Konya Türkiye

ABSTRACT

In recent years, there has been a notable increase in the number of studies utilizing three-dimensional (3D) scanners and computed tomography in the field of anatomy. However, the literature reveals that studies evaluating the compatibility between these two methods remain limited. In this study, a total of 12 adult rabbits were used. Following maceration, selected limb bones were subjected to 3D reconstruction using both computed tomography (CT) and 3D scanner. The resulting models were analyzed morphologically. On the scapula, the ventral end of the acromion was observed to terminate at the proc. hamatus and extend caudally as the metacromion. In the humerus, the tuberculum majus slightly surpassed the caput humeri, and a foramen supratrochleare was present at the distal end. The antebrachial skeleton consisted of the radius and ulna, with the ulna being more developed. The radius displayed a distinct fovea capitis radii and processus styloideus radii, while the ulna exhibited a prominent tuber olecrani and a proc. styloideus ulnae. The femur, the trochanter major extended beyond the femoral head, with the crista intertrochanterica located between the trochanter major and trochanter minor. At the distal femur, facies poplitea were clearly visible. The crural skeleton consisted of the tibia and fibula, which were fused into a single structure. In conclusion, the anatomical landmarks identified in the 3D models generated by both methods were consistent. While CT excels in scanning entire tissues and providing rapid data, 3D scanners offer advantages portability, color imaging, and cost. Combined use of methods is considered beneficial for veterinary anatomy education.

Keywords: 3D scanner, 3D reconstruction, Computed tomography, Method comparison

***

Yeni Zelanda Tavşanlarında Bazı Ekstremite Kemiklerinin 3 Boyutlu Tarayıcı ve Bilgisayarlı Tomografi ile 3 Boyutlu Rekonstrüksiyonu: Morfolojik İnceleme

ÖZ

Son yıllarda, anatomi alanında 3 Boyutlu (3B) tarayıcılar ve bilgisayarlı tomografi kullanan çalışmaların sayısında belirgin bir artış olmuştur. Ancak literatürde, bu iki yöntem arasındaki uyumluluğu değerlendiren çalışmaların sınırlı olduğu gözlenmiştir. Yapılan çalışmada toplam 12 yetişkin tavşan kullanılmıştır. Maserasyonun ardından, seçilen ekstremite kemikleri hem bilgisayarlı tomografi (BT) hem de 3B tarayıcı kullanılarak 3B rekonstrüksiyona tabi tutulmuştur. Elde edilen modeller, morfolojik olarak analiz edilmiştir. Scapula'da, acromion'un ventral ucunun proc. hamatus'ta sonlandığı ve metacromion olarak caudal olarak uzandığı gözlemlendi. Humerus'ta, tuberculum majus'un caput humeri'yi hafifçe aştığı ve distal uçta foramen supratrochleare gözlendi. Önkol iskeleti radius ve ulna'dan oluştuğu ve ulna'nın daha gelişmiş olduğu gözlendi. Radius, belirgin bir fovea capitis radii ve proc. styloideus radii sahipken, ulnae'da belirgin bir tuber olecrani ve processus styloides ulnae varlığı tespit edildi. Femur'da, trochanter major'un caput femoris düzeyini aştığı ve crista intertrochanterica trochanter major ile trochanter minor arasında yer aldığı gözlendi. Distal femurda, facies poplitea belirgindi. Ossa cruris, tek bir yapı halinde birleşmiş tibia ve fibula şeklinde olduğu tespit edildi. Sonuç olarak, her iki yöntemle oluşturulan 3B modellerde belirlenen anatomik noktalar benzerlik göstermekteydi. CT, tüm dokuları tarama ve hızlı veri sağlama konusunda üstünlük sağlarken, 3B tarayıcılar taşınabilirlik, renkli görüntüleme ve maliyet açısından avantajlar sunmaktadır. Yöntemlerin birlikte kullanılması, veteriner anatomi eğitimi için faydalı olabileceği düşünülmektedir.

Anahtar Kelimeler: 3B rekonstrüksiyon, 3B tarayıcı, Bilgisayarlı tomografi, Metot karşılaştırma

To cite this article: Koçyiğit A. Dayan MO. Koplay M. 3D Reconstruction of Some Limb Bones in New Zealand Rabbits with 3D Scanning And Computed Tomography: Morphological Investigation. Kocatepe Vet J (2025) 18(3):311-320

Submission: 13.06.2025 **Accepted**: 10.09.2025 **Published Online**: 11.09.2025
ORCID; *AK: 0000-0002-9354-7480, MOD: 0000-0003-0368-4607, MK: 0000-0001-7513-4968*
*Corresponding author e-mail: akocyigit@harran.edu.tr

INTRODUCTION

Medical imaging techniques facilitate the diagnosis, treatment and management of disease by health professionals. In the present era, techniques such as X-ray, Computed Tomography (CT), Magnetic Resonance Imaging (MRI) and ultrasound are employed with considerable frequency. In recent years, three-dimensional scanning technology with high accuracy and no negative side effects has become increasingly prevalent.

Although the foundations of three-dimensional scanning technology can be traced back to 1960, the initial generation of devices incorporated light, a single camera, and a single projection. Given the lack of technological advancement at the time, the scanning process was inherently time-consuming. Scanners that permit the detailed scanning of objects at high resolution and speed were first made available for sale in 1994 (Edl et al. 2018). Three-dimensional (3D) scanners are employed extensively in the medical domain, including human medicine (Schmalz et al. 2012), veterinary anatomy (Hackmann et al. 2019), archaeology (Remondino 2011), and dentistry (Rosicky et al. 2016). Despite the perception that the areas where techniques such as photogrammetry, laser scanners, structured light scanners and stereoscopy are used today are distinct, many scanners employ a similar underlying principle (Raja and Fernandes, 2007). The development of computed tomography (CT) technology can be traced back to the discovery of X-rays. The discovery of X-rays is generally accepted as having occurred in 1895, although its emergence can be traced back to 1850 (Mould, 1995). The first commercially available CT scanner was produced in 1972, and since then, numerous studies have been conducted on this technology. This study aims to utilise a 3D scanner and CT sections to create a 3D model of some extremity bones in New Zealand rabbits. Computed tomography is frequently used in the field of veterinary anatomy. The aim of the study is to compare the anatomical points of 3D models obtained with a 3D scanner with those obtained by computed tomography and to contribute to veterinary anatomy education.

MATERIALS and METHODS

Experimental Animal Model

In this study, six male and six female adult New Zealand rabbits were used and subsequently euthanised following the administration of general anaesthesia (Lipman et al. 1990; Oguntoye and Oke 2014; Gökmen et al. 2019). The animals were subjected to classical maceration, as described by Taşbaş (1965). Study permissions were obtained from Selçuk University Animal Experiments Local Ethics Committee (Decision no: 2020-57 (Appendix-1)).

CT Scan and 3D Modelling

In the study, a multislice spiral tomography device (Siemens Dual Source, Somatom Definition Flash, Germany) was employed for bone scans. Imaging was conducted using the following parameters: 120 kV, 300 mA, 0.6 mm slice thickness, 512 x 512 matrix. Three-dimensional modelling was conducted using the 3D Slicer 5.0.3 software.

3D Modelling with 3D Scanner Device

In the study, Shining 3D EinScan Pro 2X (2020) + Shining 3D EinScan Colour Pack was used for 3D scanning. EXScan Pro v.3.6.0.5 software was used for modelling. Device calibration was performed with an accuracy of 0.026 mm and 0.039 pixels. The process was completed by obtaining 18 images in a single scan in fixed scan mode. After the first scan was completed, the position of the bone was changed and images were obtained from different angles. Imaging was performed from four different angles. The 3D models were then obtained and exported in ".stl and .obj" formats.

RESULTS

In this study, three-dimensional models obtained from CT scans and three-dimensional scanner models were compared morphologically. The findings obtained from both methods were found to be parallel to each other.

Scapula

It was observed that the scapula was smooth, flat, and narrowed until the collum scapulae, with the dorsal part of the latter resembling a triangle. It was observed that the spina scapulae divided the bone into the fossa supraspinata and the fossa infraspinata. The fossa infraspinata was observed to narrow from the angulus caudalis to the collum scapulae. The spina scapulae was observed to ascend from dorsal to ventral, extending over the fossa infraspinata. It was observed that the spina scapulae terminated in a ventral position, in proximity to the acromion. It was established that the acromion terminates as the proc. hamatus at the ventral end of the bone and extends caudally as the metacromion. The fossa subscapularis is observed to have a wide distribution in the facies medialis. It was observed that the cavitas glenoidalis in the ventral part of the scapula resembled a gourd, narrowed by the incisura glenoidalis and bounded by the tuberculum supraglenoidale. It was established that the processus corocoideus in the cranial region of the bone exhibited a hook-shaped configuration, terminating in a bending motion towards the facies costalis (Figure 1).

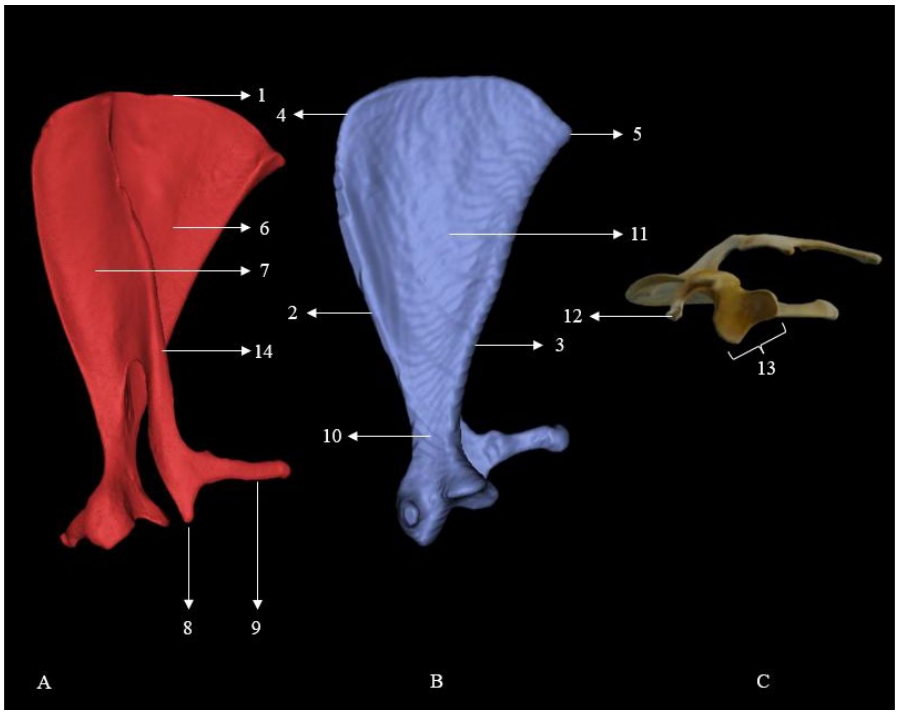

Figure 1. Reconstruction image and anatomical landmarks of the scapula. A: 3D Scanner model .stl file format; B: CT 3D model; C: 3D Scanner color scanned 3D model. 1. Margo dorsalis, 2. Margo cranialis, 3. Margo caudalis, 4. Angulus cranialis, 5. Angulus caudalis, 6. Fossa infraspinata, 7. Fossa supraspinata, 8. Acromion, 9. Metacromion, 10. Collum scapulae, 11. Fossa subscapularis, 12. Processus coracoideus, 13. Cavitas glenoidealis, 14. Spina scapulae

Humerus

The caput humeri was observed to be markedly wide. The tuberculum majus was observed in the cranio-lateral aspect of the caput humeri, while the tuberculum minus was noted in the cranio-medial aspect. The tuberculum majus exhibited a slight prominence relative to the caput humeri. The sulcus intertubercularis was observed to be situated ventrally between the tuberculum majus and the tuberculum minus. The collum humeri, situated in a ventral position relative to the caput humeri of the tuberculum majus bone, was identified. The tuberositas deltoidea, which descends ventrally from the border of the tuberculum majus located on the cranial aspect of the humerus, was observed to be relatively blunt. As the tuberositas deltoidea descended distally, the corpus became rounded and the final third of the corpus was flattened by lateral expansion, subsequently joining the trochlea humeri. The presence of articular faces, designated as the condylus medialis and condylus lateralis in the distal region of the extremity, and the trochlea humeri articulating with the ossa antebrachii in the area between these articular faces, was established. The presence of the foramen supratrochleare, which provides articulation between the fossa olecrani and the fossa radialis located distal to the extremities, was determined (Figure 2).

Ossa antebrachii

It was observed that the skeleton antebrachii was formed by the radius and ulna. The radius developed to a lesser extent than the ulna, exhibiting a broad proximal section that narrowed towards the corpus and terminated in a thickened distal section.

Radius

The radius, which exhibited a slight arching motion in a forward direction and extended to the cranio-lateral aspect of the ulna, was observed to establish contact with the ulna at both the proximal and distal regions. The caput radi exhibited two distinct fovea capitis radii, while the trochlea radii and proc. styloideus radii (medialis) were clearly discernible. The presence of the facies articularis carpeae was evident on the distal aspect (Figure 3).

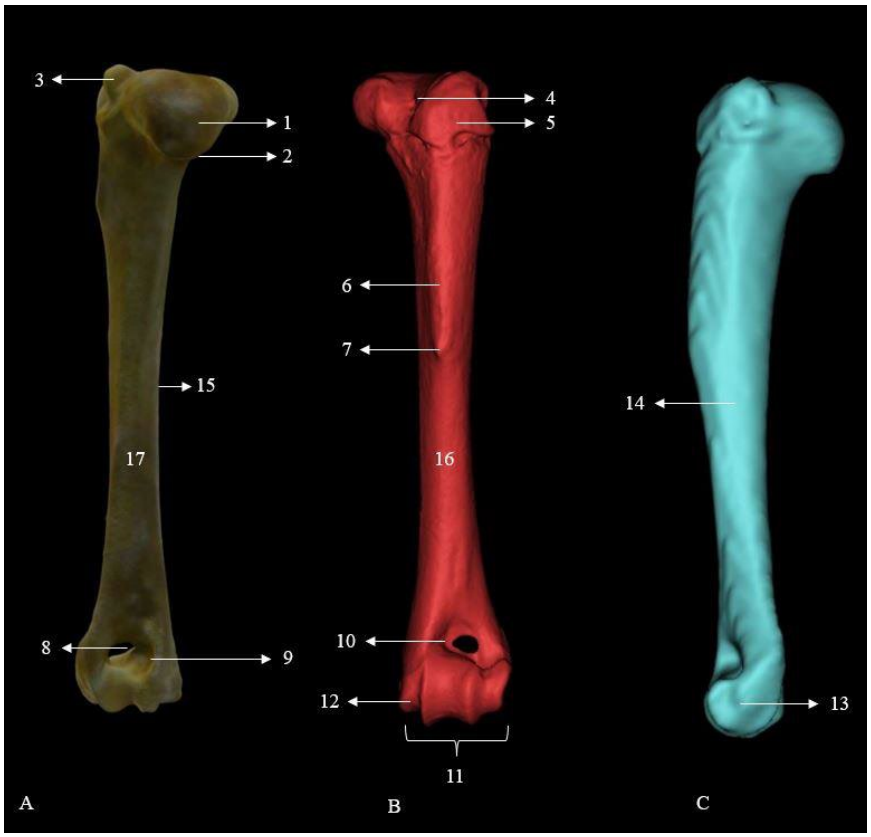

Figure 2. Reconstruction image and anatomical landmarks of the Humerus. A: 3D Scanner color scanned 3D model; 3D Scanner model .stl file format; C: CT 3D model. 1. Caput humeri, 2. Collum humeri, 3. Tuberculum majus, 4. Sulcus intertubercularis, 5. Tuberculum minus, 6. Crista humeri, 7. Tuberositas deltoidea, 8. Foramen supratrochleare, 9. Fossa olecrani, 10. Fossa radialis, 11. Trochlea humeri, 12. Epicondylus medialis, 13. Epicondylus lateralis, 14. Facies lateralis, 15. Facies medialis, 16. Facies cranialis, 17. Facies caudalis.

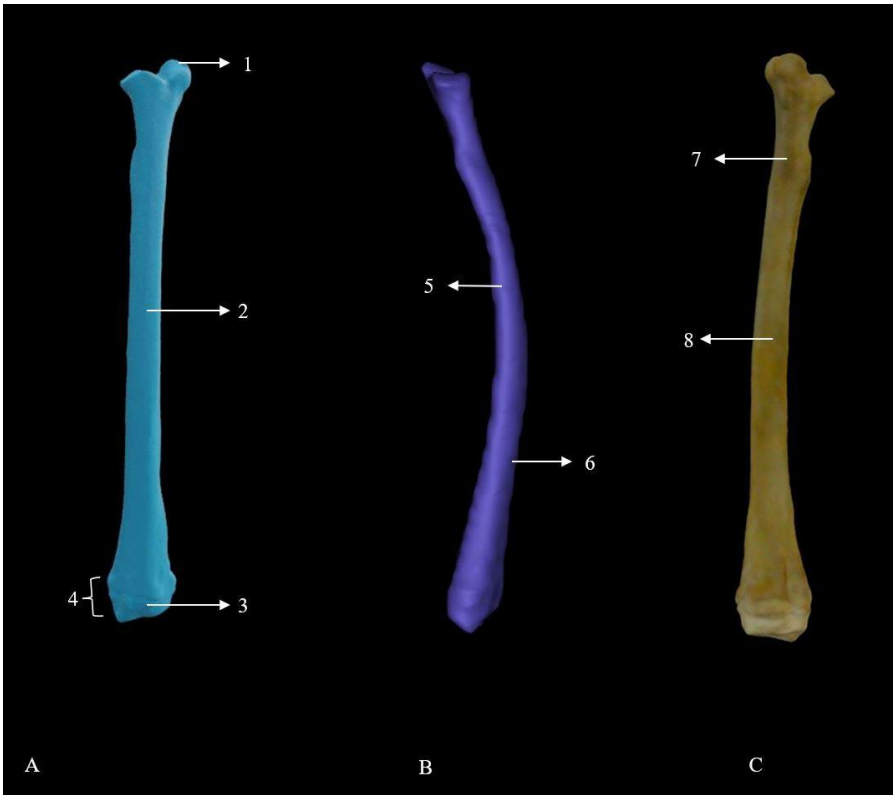

Figure 3. Reconstruction image and anatomical points of the radius. A: 3D Scanner model .stl file format; B: CT 3D model; C: 3D Scanner colour scanned 3D model. 1. Fovea capitis radii, 2. Corpus radii, 3. Proc. styloideus radii (medialis), 4. Trochlea radii, 5. Facies medialis 6. Facies cranialis, 7. Facies caudalis 8. Facies caudalis.

Ulna

In its proximal position, the bone runs caudal to the radius, while in its distal position, it is situated caudo-laterally to the radius. The proximal part of the bone is characterised by a prominent olecranon, which is terminated by three projecting tuber olecrani. The incisura trochlearis was observed to be concave, terminating proximally with the processus ancenous and distally with the processus coronoideus medialis and processus coronoideus lateralis. The incisura radialis, which separates the processus coronoideus medialis and processus coronoideus lateralis, was observed. Additionally, the corpus ulnae exhibited the presence of facies cranialis, facies medialis, and facies caudalis. Distally, the processus styloideus ulnae (lateralis) was also observed (Figure 4).

Femur

The caput femoris was observed in the proximal part of the femur, and the trochanter major was observed to be in a state of flexion, with its superior aspect extending beyond the level of the caput femoris. The fovea capitis femoris was clearly discernible on the caput ossis femoris. The femur exhibited three distinct protrusions: the trochanter major, the trochanter minor, and the trochanter tertius. A deep fossa trochanterica was observed between the caput femoris and the trochanter major, as well as a crista intertrochanterica between the trochanter major and the trochanter minor. The distal epicondyle medialis and the epicondyle lateralis were observed. The fossa intercondylaris and horizontal linea intercondylaris were observed between the two condylus. The trochlea ossis femoris was observed on the cranial aspect of the femur, allowing the patella to fit. The fossa extensoria was prominently located on the condylus lateralis. The tuberositas supracondylaris and facies poplitea were prominent (Figure 5).

Skeleton cruris

It consists of tibia and fibula. The proximal cross-sectional surface resembles a triangle. When viewed from the proximal side, it was observed that the surface was divided into two as condylus medialis and condylus lateralis and eminantia intercondylaris were located between the surfaces in the form of protrusions. Area intercondylaris centralis was present between the two eminantia intercondylaris. The presence of a tuberositas tibia was observed cranial to the bone. The tuberositas tibia was found to continue distally as crista tibia. Sulcus extentorius was found to be present. It was observed that the fibula was located caudo-lateral to the midpoint of the tibia. A wide spatium interosseum cruris was observed between the fibula and tibia. Linea m. poplitei was prominent. It was observed that the cochlea tibia located in the distal extremities was rectangular, parallel to the medial axis, and had prominent malleolus lateralis and malleolus medialis projections (Figure 6).

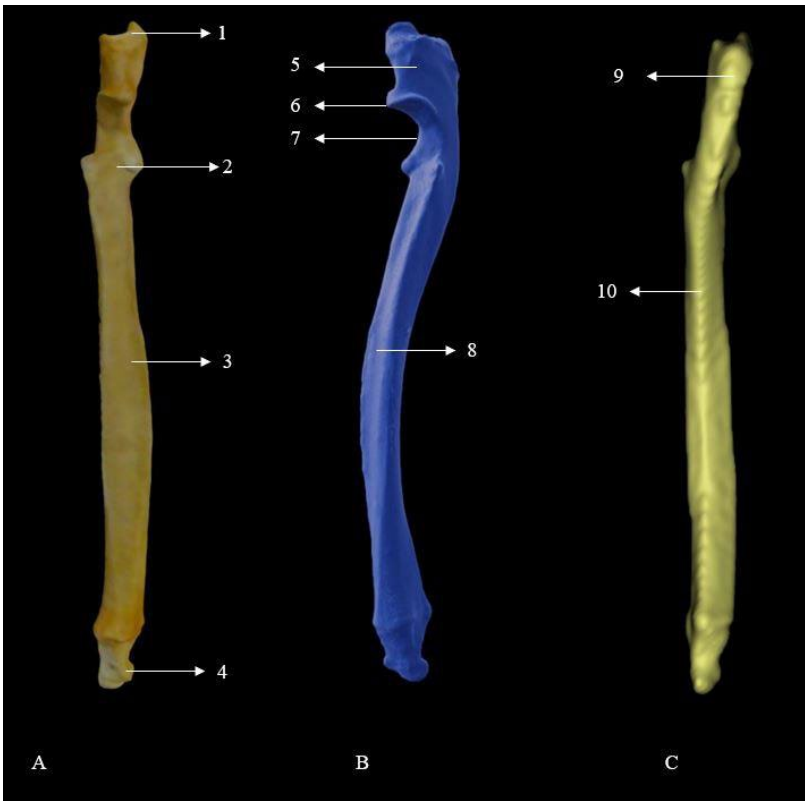

Figure 4. Reconstruction image and anatomical points of the ulna. 3D Scanner colour scanned 3D model; B: 3D Scanner model .stl file format; C: CT 3D model. 1. Tuber olecrani, 2. Proc. coronideus medialis ve lateralis, 3. Corpus ulnae, 4. Proc. styloideus ulnae (lateralis), 5. Olecranon, 6. Proc. anconeus, 7. Incisura trochlearis, 8. Margo lateralis, 9. Margo caudalis. 10. Facies caudalis.

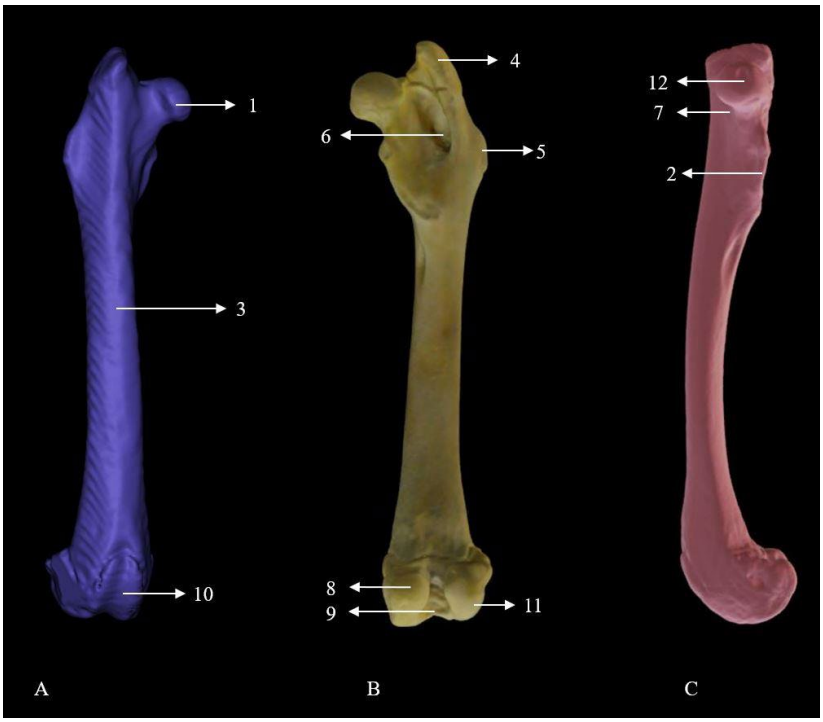

Figure 5. Reconstruction image and anatomical points of the femur.A: 3D Scanner colour scanned 3D model; B:3D Scanner model in .stl file format; C: CT 3D model. 1. Caput femoris, 2. Trochanter minus, 3. Corpus ossis femoris, 4. Trochanter major, 5. Trochanter minor, 6. Fossa intertrochanterica, 7. Collum femoris, 8. Condylus medialis, 9. Fossa intercondylaris, 10. Trochlea femoris, 11. Condylus lateralis, 12. Fovea capitis femoris.

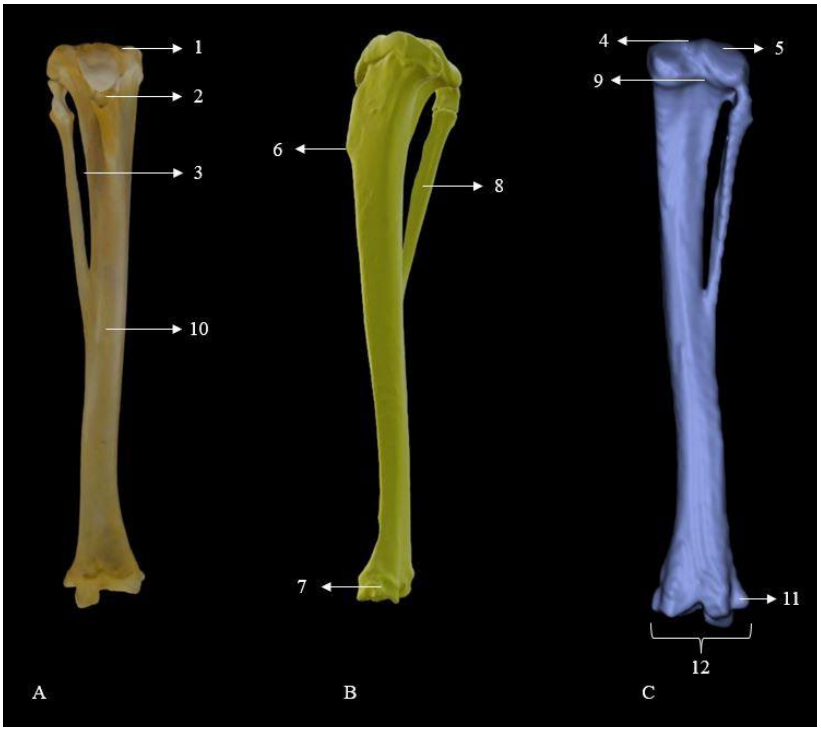

Figure 6. Reconstruction image and anatomical points of the skeleton cruris. A: 3D Scanner colour scanned 3D model; B: 3D Scanner model in .stl file format; C: CT 3D model. 1. Condylus medialis, 2. Tuberositas tibia, 3. Spatium interosseum cruris, 4. Eminentia intercondylaris, 5. Condylus lateralis, 6. Crista tibiae, 7. Malleolus medialis, 8. Fibula, 9. Inc. Poplitea, 10. Corpus tibiae, 11. Malleolus lateralis, 12. Cochlea tibiae.

DISCUSSION

3D models are used in many different fields, including the medical field, and their use in veterinary anatomy and anatomy education has become widespread in recent years. In the studies conducted, the models obtained using 3D scanners are physically printed by 3D printers and used as teaching materials and in areas such as plates and fixators in surgical procedures. Software can be used to take measurements and make adjustments on the models.

Tomography slices assist physicians in the diagnosis, detection and treatment of diseases. In recent years, 3D models have been created using tomography slices, providing us with more information about the scanned tissue, enabling us to take measurements and obtain preliminary information for surgical operations.

The scapula is the first bone connected to the body by muscles. In a study conducted on wild rabbits and domestic rabbits, it was found that the scapula is a flat bone consisting of lateral and medial surfaces and forms a joint with the cavitas glenoidalis, which is consistent with the findings of the study (Hussein Al-Ubaidy et al. 2020).

It has been reported that the scapula in rats (Salami et al. 2011) and rabbits (El-Ghazali and El-Behery 2018) is triangular in shape, while in marsupials, there are two types: triangular and quadrangular (Argot 2001). The models obtained show that the scapula is triangular in shape, which is consistent with the literature (Barone 1986). In a study conducted on wombats (Saber 2013), it was determined that the fossa infraspinata is wider than the fossa supraspinata in models obtained from both methods (El-Ghazali and El-Behery 2018). The spina scapulae, which starts between the two fossae and continues to rise to the level of the cavitas glenoidalis, ending at the acromion and continuing caudally as the metacromion, is consistent with the literature (Chin Jr 1957; El-Ghazali and El-Behery 2018; Doubell et al. 2020). The protrusion located on the lateral part of the scapula, called the metacromion, which continues caudally in a narrow and long shape, was clearly observed in the study. It has been reported that the muscles attached to this protrusion assist in the extension of the arm (Seckel and Janis 2008; El-Ghazali and El-Behery 2018). The cavitas glenoidalis was observed to be wide, developed in accordance with the surface of the caput humeri , and consistent with the literature (El-Ghazali and El-Behery 2018). The authors reported that the incisura glenoidalis was not detected in the study conducted on cats, but was present in the studies conducted on the African giant pouched rat (Cricetomys gambianus) and mole-rat (Özkan 2002a; Olude et al. 2010; Yılmaz et al. 2020a). In the present study, the incisura glenoidalis was clearly observed. In a study conducted on the wombat (Saber 2013), the cavitas glenodealis was reported to be oval in shape, while in studies conducted on the African giant rat (Cricetomys gambianus) (Olude et al. 2010) and squirrel (Kazeem et al. 2020), the processus coroideus was reported to be hook-shaped. Similar findings were observed in the models obtained in the present study.

Studies conducted on rabbits, guinea pigs, mongooses (Shunmugam and Sundaram 2022), Van cats (Yılmaz et al. 2020b), agoutis (Sundaram et al. 2015), and wild cats (Palanisamy et al. 2020) reported the presence of a distinct caput humeri, tuberculum majus, and tuberculum minus were reported by the authors. Shunmugam and Sundaram (2022) reported the presence of the caput humeri, tuberculum majus, tuberculum minus, and sulcus intertubercularis on the humerus in rabbits, guinea pigs, and Egyptian mice in their comparative study. Chiarello et al. (2021) reported the presence of the greater tubercle and lesser tubercle in opossums, along with a wide sulcus intertubercularis separating them. In wombats, the greater tubercle is divided into the cranial and caudal parts, and the presence of a very prominent deltoid tuberosity has been reported (Saber 2013). In the 3D models obtained, the tuberculum majus slightly exceeded the caput humeri, was separated from the tuberculum minus by the sulcus intertubercularis, and a less prominent tuberositas deltoidea was observed. In studies conducted on different species such as guinea pig (Witkowska et al. 2014, Shunmugam and Sundaram 2022), wombat (Saber 2013), African giant rat (Olude et al. 2010), Coypu (Şeicaru 2019), porcupine (Hystrix Cristata) (Yılmaz et al. 1998), mongoose (Shunmugam and Sundaram 2022) in the distal part of the humerus, it has been reported that the trochlea humeri consists of the lateral epicondyle and the medial epicondyle, and that the foramen supratrochleare, which connects the fossa radialis and the fossa olecrani, is located above these anatomical structures. In the present study, it was determined that the trochlea humeri consists of the condylus lateralis and condylus medialis, and that the supratrochlear foramen is located above these condyles and connects the fossa olecrani and the fossa radialis.

It was determined that the forearm consists of two bones, the radius and ulna, and that the ulna is more developed than the radius. It has been reported that the radius is concave towards the cranium and that the fovea capitis radii is located in its proximal section for the humerus joint surface to fit (El-Ghazali and El-Behery 2018, Akgün et al. 2021). The styloid process of the radius located at the distal end of the bone is consistent with the literature (Chin Jr 1957). The olecranon, which is clearly observed in studies conducted on wombats, cats, rats, and giant rats, is located in the proximal section of the ulna, which is more developed than the radius. The tuber olecrani, which ends proximal to the olecranon, and the proc. ancenous, and the inc. trochlearis, where the ulna articulates with the humerus, are reported by the authors (Saber 2013). In the three-dimensional models obtained in the study, the tuber olecrani was found to

have three protrusions, and the olecranon, incisura trochlearis, and processus ancenous were clearly observed in both methods (Yılmaz et al. 1998, El-Ghazali and El-Behery 2018, Yılmaz et al. 2020b). It was determined that the ulna terminates distally with the of the processus styloideus ulnae (Van Staden 2014).

Bakici et al. (2021) reported in their study on rabbits using micro-CT sections that the trochanter majör exceeded the level of the femoral head, the trochanter minor and the trochanter tertius were at the same level, and there was a deep fossa trochanterica (Bakıcı et al 2021). Using magnetic resonance imaging, it was reported that the rabbit femur has a caput femoris, trochanter major, trochanter minor, trochanter minor, and a deep fossa trochanterica (Wang et al 2009). In mole-rat, the authors reported the presence of the trochanter major, trochanter minor, trochanter tertius, and a deep fossa trochanterica, along with the crista intertrochenterica, and additionally, the presence of the fovea capitis in mole-rat (Özkan 2002b; Özkan 2002c). The absence of the trochanter tertius in chinchillas and the fovea capitis in African giant rats has been reported (Çevik-Demirkan et al. 2007; Olude et al. 2023). In studies conducted on different rodent species (de Araújo et al. 2013) and the African giant rat (Olude et al. 2023), as well as the chinchilla (Çevik-Demirkan et al 2007), it was reported that the distal part of the femur is divided into two parts, the lateral and medial condyles, with the intercondylar fossa between them, and that the lateral epicondyle and medial epicondyle were observed for muscle attachment, which is consistent with the findings of the present study. A distinct extensor fossa was identified on the trochanteric fossa and lateral condyle in the cranial part of the distal region.

The ossa cruris, consisting of the tibia and fibula, assist in stabilising the foot and, depending on the fusion status of the fibula, are thought to contribute to ankle movement. (Polly and Hall, 2007). In studies conducted on cats and chinchillas, the authors reported that the proximal section of the tibia is triangular and that the fibula develops separately (Çevik-Demirkan et al. 2007; El-Ghazali and El-Behery 2018). In burrowing species, the tibia and fibula fuse, and this is thought to contribute to bone strength, preventing bending during digging (Montoya-Sanhueza et al. 2022). Studies on rats (Salami et al. 2011), African mole-rats (Sahd et al 2019), and hedgehogs (Girgiri et al. 2016) have reported that the fibula fuses with the tibia. It was found that the tibia takes on a rectangular shape distally and that the cochlea tibia is in a sagittal position and consists of two parts, which is consistent with the literature (El-Ghazali and El-Behery 2018).

3D scanners have advantages in areas where tomography and MR scanners cannot be used because they are portable, inexpensive, and obtain data in color from the scanned surface (Wilhite and Wölfel 2019, da Silveira et al 2021). It has disadvantages compared to medical imaging devices due to modeling time and scanning only the surface (Wilhite and Wölfel 2019).

CONCLUSION

In this study, 3D reconstruction of some selected bones was performed using CT and 3D scanner. Both 3D scanner and CT results were observed, showing that different methods can be used in the field of veterinary anatomy. In addition to the advantages of the 3D scanner device, such as low sensitivity and high resolution, the fact that it can produce models in color, that it produces models quickly and efficiently, and that the 3D surface models and morphometric measurements obtained are closely related to tomography, have proven that 3D scanners can be used in the field of veterinary anatomy. We believe that the models obtained from 3D scanners will make important contributions to the teaching of veterinary anatomy by creating virtual models in color and printing them with 3D printers. Traditional textbooks may not be sufficient to understand the relationship between anatomical structures because they contain 2-dimensional images. Cadavers are time-consuming, limited in number, and not always available due to ethical concerns. 3D models fill these gaps. In this study, 3D scanning may be preferred because it is less expensive than tomography, is portable, can scan in free mode, has a lower margin of error, is easy to use, has no access limitations compared to medical imaging modalities such as CT and MRI, allows modeling of soft tissues, produces high-resolution 3D models, has no harmful side effects, and can scan in color. As a result of the study, we believe that the two methods should be integrated in use.

Conflict of interest: The authors have no conflicts of interest to report.

Authors' Contributions: AK and MOD contributed to the project idea, design and execution of the study. AK, MOD contributed to the acquisition of data. AK analysed the data. AK and MOD drafted and wrote the manuscript. AK, MOD and MK reviewed the manuscript critically. All authors have read and approved the finalized manuscript.

Ethical approval: Study permissions were obtained from Selçuk University Animal Experiments Local Ethics Committee (Decision no: 2020-57 (Appendix 1)).

Acknowledgement This research was supported by Selçuk University Scientific Research Project Coordination Office with the project number "21212006".

Explanation: *This article is summarized from the PhD thesis.

REFERENCES

Akgün, R.O., Orhan, İ. Ö., & Okan, E. (2021). Three-dimensional bone modeling of forelimb joints in New Zealand Rabbit: A Micro-Computed Tomography study. Ankara Universitesi Veteriner Fakultesi Dergisi, 68, 4, 355-63. https://doi.org/10.33988/auvfd.762615

Al-Ubaidy, A. A. H., Jabbar, A. I., & Al-Agele, R. A. A. (2020). Morphometric comparative study of scapula as example of shoulder girdle and os coxa as example of pelvic girdle in hare and domesticated rabbit. EurAsian Journal of BioSciences, 14, 5093-5. e-ISSN: 1307-9867

Argot, C. (2001). Functional-adaptive anatomy of the forelimb in the Didelphidae, and the paleobiology of the Paleocene marsupials Mayulestes ferox and Pucadelphys andinus. Journal of Morphology, 247, 1, 51-79. https://doi.org/10.1002/1097-4687(200101)247:1<51::AID-JMOR1003>3.0.CO;2-%23

Bakici, C., Akgun, R., Ekim, O., Batur, B., Bakici., M., Ozen., D., & Soydal., C. (2021). Three dimensional modeling and quantitative analysis of long bone parameters of rabbit using micro-computed tomography. Iranian Journal of Veterinary Research, 22, 2, 140. https://doi.org/10.22099/ijvr.2021.39092.5688

Barone, R. (1986). Anatomie comparée des mammifères domestiques. Tome 1: Ostéologie, Paris, Vigot Freres, p. 33-733. ISBN-13: 978-2711491605

Chiarello, G. P., Gomes, S. P., Sasahara, T. H. D. C, & Miglino, M. A. (2021). Anatomical characteristics of the bones of the thoracic limb of white-eared opossum (Didelphis albiventris). International Journal of Morphology, *39*(2), 416-422. https://doi.org/10.4067/S0717-95022021000200416

Chin, Jr, E. (1957). The rabbit: an illustrated anatomical guide. Master's Thesis, College of the Pacific.

Çevik-Demirkan, A., Özdemir, V., Türkmenoğlu, İ., & Demirkan, I. (2007). Anatomy of the hind limb skeleton of the chinchilla (Chinchilla lanigera). Acta Veterinaria Brno, 76, 4, 501-7. https://doi.org/10.2754/avb200776040501

da Silveira, E. E., da Silva, Lisboa, Neto, A. F., Carlos, Sabino, Pereira, H., Ferreira, J. S., Dos Santos, A. C., Siviero, F., & de Assis Neto, A.C. (2021). Canine skull digitalization and three-dimensional printing as an educational tool for anatomical study. Journal Of Veterinary Medical Education, 48, 6, 649-55. https://doi.org/10.3138/jvme-2019-0132

de Araújo, F., Sesoko, N., Rahal, S. C., Teixeira, C. R., Müller T. R., & Machado M. R. F. (2013). Bone morphology of the hind limbs in two caviomorph rodents. Anatomia, Histologia, Embryologia, 42, 2, 114-23. https://doi.org/10.1111/j.1439-0264.2012.01172.x

Doubell, N. S., Sahd, L., & Kotzé, S. H. (2020). Comparative forelimb morphology of scratch-digging and chisel-tooth digging African mole-rat species. Journal of Morphology, 281, 9, 1029-46. https://doi.org/10.1002/jmor.21229

Edl, M., Mizerák, M., & Trojan, J. (2018). 3D laser scanners: History and applications. Acta Simulatio, 4, 4, 1-5. https://doi.org/10.22306/asim.v4i4.54

El-Ghazali, H., & El-Behery, E., (2018). Comparative macro-anatomical observations of the appendicular skeleton of New Zealand rabbit (Oryctolagus cuniculus) and domestic cat (Felis domestica) thoracic limb. International Journal of Veterinary Science, 7, 3, 127-33. https://www.ijvets.com/pdf-files/Volume-7-no-3-2018/127-133.pdf

Girgiri, I. A., Yahaya, A., Gambo, B. G., Majama, Y. B., & Sule A. (2016). Osteomorphology of the appendicular skeleton of four-toed african hedgehogs (Atelerix albiventris) Part (2): Pelvic limb. Global Veterinaria, 16, 413-8. https://doi.org/10.5829/idosi.gv.2016.16.05.10352

Gökmen, S., Pehlivan, A., Aksoy, A. (2019). Laboratuvar Hayvanlarında Ötenazi Yöntemleri. Etlik Veteriner Mikrobiyoloji Dergisi, 30, 1, 87-94. https://doi.org/10.35864/evmd.586565

Hackmann, C. H., Dos, Reis, D. A., de-Assis-Neto, A. C. (2019). Digital revolution in veterinary anatomy: confection of anatomical models of canine stomach by scanning and three-dimensional printing (3D). International Journal of Morphology, 37, 2, 486-90. https://doi.org/10.4067/S0717-95022019000200486

Hussein, Al-Ubaidy, A. A., Jabbar, A. I., Abood, Al-Agele, R. A. (2020). Morphometrie comparative study of scapula as example of shoulder girdle and os coxa as example of pelvic girdle in hare and domesticated rabbit. EurAsian Journal of BioSciences, 14, 2, 5093-95. ISSN: 1307-9867

Kazeem, E. O., Oyewole, O. J., Ifukot, U. L. (2020). Gross anatomical features and osteometric variables of the scapula of the african tree squirrel (Funisciurus anerythrus), house (Rattus Rattus) and wistar rats. Anatomy Journal of Africa, 9, 2, 1773-81. https://doi.org/10.4314/aja.v9i2.198923

Lipman, N., Marini, R., Erdman, S. (1990). A comparison of ketamine/xylazine and ketamine/xylazine/acepromazine anesthesia in the rabbit. Laboratory animal science, 40, 4, 395-8. PMID: 2166867

Montoya-Sanhueza, G., Šaffa, G., Šumbera, R., Chinsamy, A., Jarvis, J.U., Bennett, N., C. (2022). Fossorial adaptations in African mole-rats (Bathyergidae) and the unique appendicular phenotype of naked mole-rats. Communications Biology, 5, 1, 1-13.

Mould, R. (1995). Röntgen and the discovery of X-rays. The British journal of radiology, 68, 815, 1145-76. https://doi.org/10.1259/0007-1285-68-815-1145

Oguntoye, C., Oke, B. (2014). A comparison of xylazine/ketamine, diazepam/ketamine and acepromazine/ketamine anaesthesia in rabbit. Sokoto Journal of Veterinary Sciences, 12, 3, 21-5. https://doi.org/10.4314/sokjvs.v12i3.4

Olude, M. A., Olopade, J. O., Akinloye, A. K., Mustapha, O. A. (2010). Macro-anatomical investigations of the skeletons of the African giant rat (Cricetomys gambianus Waterhouse 1840) II: Fore limb. Eur J Anat, 14, 1, 19-23. ISSN: 2340-311X

Olude, M.A, Olopade, J.O., Mustapha, O.A. (2023). Macro-anatomical investigations of the skeletons of the African giant rat (Cricetomys gambianus Waterhouse): Pelvic limb. European Journal of Anatomy, 13, 3, 127-31.

Özkan, Z. E. (2002a). Macro-anatomical investigations on the forelimb skeleton of mole-rat (Spalax leucodon Nordmann). Vet. arhiv 72, 91-99, 2002.

Özkan, Z. E. (2002b). Macro-anatomical investigations on the hind limb skeleton of mole-rat (Spalax leucodon Nordmann). Veterinarski Arhiv, 72(3), 159-166.

Özkan, Z. E. (2002c). Macro-anatomical investigations on the skeletons of hedgehog (Erinaceus europaeus L.). II. Ossa membri pelvini. Veterinarski arhiv, 72, 4, 213-20. ISSN**:** 0372-5480

Palanisamy, D., Tomar, M., Ankem, P. B., Sekhar, R. (2020). Humerus of Indian Wildcat (Felis silvestris ornata: Gray, 1830)—A Gross Osteological Study. International Journal of Livestock Research, 10, 49-54. http://dx.doi.org/10.5455/ijlr.20200211041708

Polly, P. D., Hall, B. (2007). Limbs in mammalian evolution. Fins into limbs: evolution, development and transformation, 245-68. ISBN: 9780226319942

Raja, V., Fernandes, K. J. (2007). Reverse engineering: an industrial perspective, Springer Science & Business Media, p. 1-115. http://dx.doi.org/10.1007/978-1-84628-856-2

Remondino, F. (2011). Heritage recording and 3D modeling with photogrammetry and 3D scanning. Remote sensing, 3, 6, 1104-38. http://dx.doi.org/10.3390/rs3061104

Rosicky, J., Grygar, A., Chapcak, P., Bouma, T., et al. (2016). Application of 3D scanning in prosthetic & orthotic clinical practice. Proceedings of the 7th international conference on 3D body scanning technologies, 88-97. http://dx.doi.org/10.15221/16.088

Saber, A. S. M. (2013). Some morphological observations on the thoracic limb bones of the Hairy-Nosed Wombat (Lasiorhinus latifornis, Owen). Journal of Veterinary Anatomy, 6, 2, 93-109. http://dx.doi.org/10.21608/jva.2013.45026

Sahd, L., Bennett, N. C., Kotzé, S. (2019). Hind foot drumming: morphological adaptations of the muscles and bones of the hind limb in three African mole-rat species. J Anat, 235, 4, 811-24. http://dx.doi.org/10.1111/joa.13028

Salami, S.O., Onwuama, K.T., Maidawa, M.S., Imam, J., Ojo, S.A. (2011). Morphological studies of the appendicular skeleton of the African giant pouched rat (Cricetomys gambianus) Part (1) pectoral limb. Journal of veterinary medicine and animal health, 3, 7, 82-7.

Schmalz, C., Forster, F., Schick, A., Angelopoulou, E. (2012). An endoscopic 3D scanner based on structured light. Medical image analysis, 16, 5, 1063-72. http://dx.doi.org/10.1016/j.media.2012.04.001

Seckel, L., Janis, C. (2008). Convergences in scapula morphology among small cursorial mammals: an osteological correlate for locomotory specialization. Journal of Mammalian Evolution, 15, 4, 261-79.

Shunmugam, R., Sundaram, M. (2022). Comparative Morphology of the Humerus of Rabbit, Guinea Pig and Mongoose. Indian J Vet Sci Biotechnol, 18, 4, 59-63. e-ISSN**:** 2395-1176

Sundaram, V., Dumas, N., Adogwa, A., Rao, S., Nayak, S.B., (2015). Morphological studies of the forelimb skeleton of the orange rumped agouti (Dasyprocta leporina Linnaeus, 1758). Annual Research & Review in Biology, 1-9.

Şeicaru, A. (2019). Biodiversity of the thoracic limb skeleton in Coypu. Scientific Works Series C. Veterinary Medicine, LXV, 2, 11-6.

Taşbaş, M. (1965). Maserasyon tekniği üzerinde araştırmalar. Ankara Univ Vet Fak Derg, 12(04), 325-330. e-ISSN: 1308-2817

Van Staden, S. L. (2014). The thoracic limb of the suricate (Suricata suricatta): osteology, radiologic anatomy, and functional morphologic changes. J Zoo Wildl Med, 45, 3, 476-86. http://dx.doi.org/10.1638/2012-0280R1.1

Wang, H-H., Wang, Y-X., J., Sheng, H., Zhang, G., Qin, L., Ahuja, A.T., Teng, L-S. (2009). Fossa trochanterica of the proximal femur in rabbits: an anatomic structure for potential misinterpretation on magnetic resonance images. Acta Radiologica, 50, 2, 212-6.

Wilhite, R., Wölfel, I. (2019). 3D Printing for veterinary anatomy: An overview. Anat Histol Embryol, 48, 6, 609-20. http://dx.doi.org/10.1111/ahe.12502

Witkowska, A., Alibhai, A., Hughes, C., Price, J., Klisch, K., Sturrock, C. J., Rutlandet C. S. (2014). Computed tomography analysis of guinea pig bone: architecture, bone thickness and dimensions throughout development. PeerJ, 2, e615. http://dx.doi.org/10.7717/peerj.615

Yılmaz, O., Soygüder, Z., Yavuz, A. (2020a). Three-Dimensional Investigation by Computed Tomography of the Clavicle and Scapula in Van Cats. Van Vet J, 31, 1. http://dx.doi.org/10.36483/vanvetj.644080

Yılmaz, O., Soygüder, Z., Yavuz, A. (2020b). Van Kedilerinde Humerus ve Antebrachium'un Bilgisayarlı Tomografi ile Anatomik, Morfometrik ve Volümetrik Olarak İncelenmesi. Harran Univ Vet Fak Derg, 9, 2, 161-9. http://dx.doi.org/10.31196/huvfd.792943

Yılmaz, S., Özkan, Z. E., Özdemir, D. (1998). Oklu Kirpi (Hystrix cristata) iskelet sistemi üzerinde makro-anatomik araştırmalar. I. Ossa membri thoracici. Turk J Vet Anim Sci, 22, 4, 389-92. ISSN: 1300-0128